Modification of edge mode dynamics by oxidation in $Ni_{80}Fe_{20}$ thin film edges

M. Zhu[1,2,*] and R. D. McMichael[3,†]

[1]Center for Nanoscale Science and Technology, National Institute of Standards and Technology, Gaithersburg, Maryland 20899, USA.
[2]Maryland Nanocenter, University of Maryland, College Park, Maryland 20742, USA
[3]Center for Nanoscale Science and Technology, National Institute of Standards and Technology, Gaithersburg, MD, 20899, USA.
(Dated: Accepted March 25, 2010)

We use "edge mode" ferromagnetic resonance (FMR) to probe the magnetic properties of oxidized $Ni_{80}Fe_{20}$ (Py) nanostripe edges. The oxidation is carried out using either oxygen plasma or thermal annealing in an oxygen ambient. We find that for both treatments the edge saturation field decreases systematically with increasing oxidation due to reduced magnetization near the edges. However, the change of effective out-of-plane anisotropy field shows opposite trends for these two oxidation methods. Micromagnetic simulations suggest that thermally annealed samples may have an additional reduction in the bulk magnetization, possibly due to a compositional change in Py stripes. The two distinct oxidation profiles also result in different changes in resonance linewidth from which we find little damping change for plasma treatment but an enhanced effective damping for thermal annealing.

I. INTRODUCTION

As the dimensions of magnetic storage devices scale down to the sub-micron level, the properties of thin film edges start to play an essential role in the magnetic behaviors of patterned devices[1–3]. Studies have shown that a sidewall oxide layer adversely affects the thermal stability of spin-torque nanomagnet devices[4], while edge oxidation in magnetic tunnel junctions was found to reduce the switching field distributions[5]. In modern nanofabrication processes, oxygen plasma etching/cleaning and thermal annealing are some inevitable steps in fabricating magnetic recording read head[6] and magnetic random access memory[7]. These steps may involve unintentional oxidation of the film edges. However, the effect of edge oxidation on magnetic properties of film edges is yet to be determined.

Previous studies of edge mode dynamics in $Ni_{80}Fe_{20}$ (Py) stripes have shown that the "trapped spin wave"[8,9] detected by ferromagnetic resonance (FMR) is a powerful way to probe the magnetic properties of Py thin film edges[10,11]. In this paper, we use this edge mode FMR technique to probe the magnetic properties of Py nanostripe edges that have been subjected to oxygen plasma or thermal oxidation processes.

II. EXPERIMENT

Py nanostripes with a structure of 3 nm Ta/ 20 nm Py/ 5 nm Al_2O_3 were fabricated by interference lithography, e-beam evaporation, and lift-off, using a trilayer resist stack mask (Fig. 1a). The trilayer stack was comprised of 90 nm antireflective coating (ARC), 30 nm SiO_2 and 400 nm photoresist, which were sequentially spun on or sputtered on a Si substrate[12]. The photoresist was exposed using laser interference lithography at a wavelength of 405 nm, and developed to form a grating pattern in the resist. Then reactive ion etching of SiO_2 was

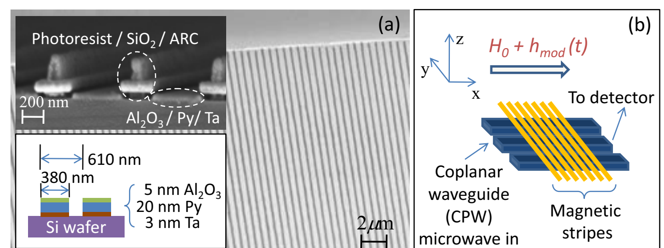

FIG. 1: (Color online) (a) Scanning Electron Microscopy (SEM) image of the nanostripes. The SEM image in the inset shows the cross-section of the stripes before the trilayer stack mask was removed. The cartoon in the inset illustrates the stripe structure. (b) Illustration showing the experiment setup and measurement configuration. H_0 is the quasi-static field and h_{mod} is an ac modulation field at 71 Hz.

used to transfer the stripe pattern to the SiO_2 layer. Oxygen plasma etching followed to partially remove the ARC layer, forming a T-shaped mask to facilitate lift-off. Finally, a uniform array of stripes with a width of ≈ 380 nm and a pitch of ≈ 610 nm was obtained by evaporation and lifting-off the stack mask.

A number of sample pieces were cut from one wafer and oxidized using either oxygen plasma or thermal annealing. Four pieces were subjected to oxygen plasma with a pressure of 26.7 Pa (200 mTorr) and an oxygen flow of 6.7×10^{-7} m^3/s (40 standard cubic centimeters per minute (sccm)). These parameters are typical for oxygen plasma etching/descumming process. The radio-frequency (RF) power was fixed at 400 W and the oxidation time was varied from 1 min to 10 min. The Al_2O_3 capping layer can effectively protect the Py top surface from plasma oxidation[13], and as a result, we expect that only the edges are exposed to the oxygen ions. Three other pieces were thermally oxidized at temperatures from 100 °C to 300 °C for 15 min, in an oxygen

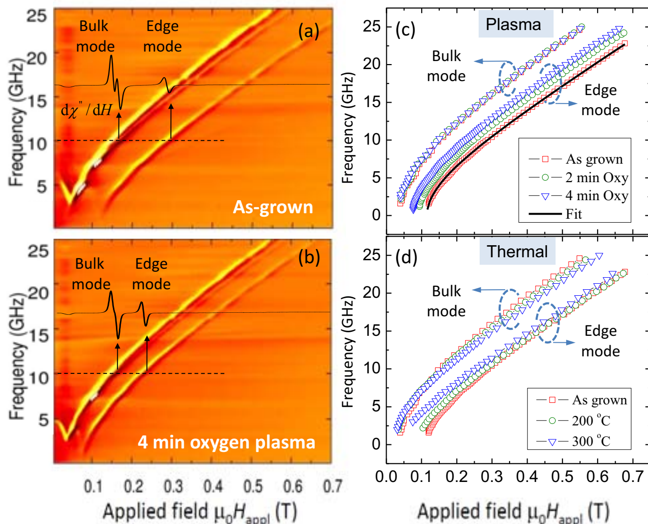

FIG. 2: (Color online) FMR spectra map for (a) as-grown sample and (b) the sample treated with 4 mins oxygen plasma. The FMR spectra at 10 GHz are shown as thick lines overlaying on the map. Edge and bulk mode frequency as a function of field for (c) samples with different plasma oxidation time and (d) samples with different annealing temperatures.

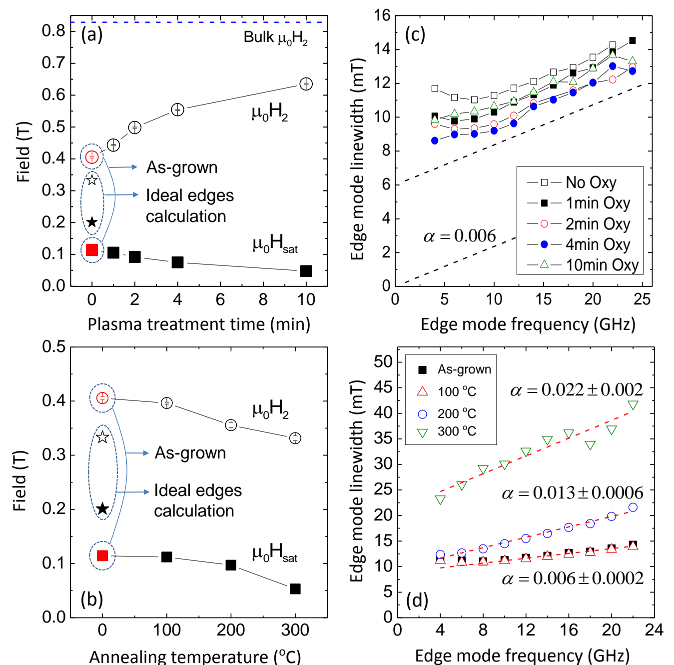

FIG. 3: (Color online) (a) $\mu_0 H_{\mathrm{sat}}$ and $\mu_0 H_2$ vs plasma oxidation time. Dashed line is the $\mu_0 H_2$ value for as-grown bulk modes. (b) $\mu_0 H_{\mathrm{sat}}$ and $\mu_0 H_2$ vs annealing temperature. The error bars in (a) and (b) are less than the symbol size. The model calculations of an ideal 20 nm thick, 500 nm wide stripe are also shown as star symbols. (c) Edge mode linewidth vs resonance frequency for plasma oxidation. Dashed lines correspond to a damping parameter of 0.006. (d) Edge mode linewidth vs resonance frequency for thermal oxidation. Dashed lines are linear fits.

flow of 1.67×10^{-5} m^3/s (1000 sccm).

The dynamic properties of the stripe edges were measured by placing the nanostripes face down on a coplanar waveguide (CPW) with a quasi-static field H_0 applied perpendicular to the stripes (Fig. 1b). At each selected microwave excitation frequency f of the CPW, the FMR modes were detected as a reduction of transmitted energy of the CPW when sweeping the field H_0. A modulation field h_{mod} with lock-in detection was also used to improve the signal to noise ratio[14].

III. RESULTS AND DISCUSSION

Fig. 2 and Fig. 3 summarize the measurement results for both plasma oxidation and thermal oxidation. Figs. 2a and 2b show an example of the FMR intensity maps for the as-grown nanostripes and the stripes subjected to 4 min of oxygen plasma respectively. The overlayed curves show the FMR spectra at 10 GHz, where two resonance modes are clearly seen. The resonance at lower and higher field for a fixed frequency are identified as the bulk mode and the edge mode respectively[14]. Compared to the bulk modes, the edge modes are shifted to higher field as a result of a reduction of internal field near the edges that is sensitive to edge profile and edge magnetization dilution[11]. The most striking change between Fig. 2a and Fig. 2b is that the edge mode for the oxidized sample moves to lower field while the bulk mode resonance barely shifts. A subtler change is that the linewidth of the edge mode resonance is also affected by oxidation. In the following, we describe analysis of the edge mode resonance and linewidth for different oxidation conditions.

For both oxidation treatments, the edge mode consistently shifts to lower field with increasing degree of oxidation as shown in Fig. 2c and 2d. To quantitatively characterize the mode behavior, we fit the field dependent edge mode frequency to a modified Kittel's FMR formula[11]:

$$f = \frac{\gamma}{2\pi}\mu_0[(H_0 - H_{\mathrm{sat}})(H_0 + H_2)]^{1/2}, \tag{1}$$

where $\gamma/2\pi$ is the gyromagnetic ratio which we fix at 29.3 GHz/T, the fitting parameter H_{sat} represents the field at which the edge magnetization is saturated perpendicular to the edges, and H_2 is an effective out-of-plane anisotropy field. The black line in Fig. 2c shows an example of such a fit for the as-grown stripes. All the reported uncertainties were obtained from the standard errors in the fitting. The uncertainties in $\mu_0 H_{\mathrm{sat}}$ and $\mu_0 H_2$ are generally less than 5 mT.

For plasma oxidized samples, we plot the obtained $\mu_0 H_{\mathrm{sat}}$ and $\mu_0 H_2$ (μ_0 is the permeability of free space) in Fig. 3a as a function of oxidation time. A decrease of edge saturation field by more than a factor of two

is found as plasma oxidation time increases, while H_2 consistently increases. However, the thermally annealed samples show a different behavior in that both $\mu_0 H_{\rm sat}$ and $\mu_0 H_2$ decrease with annealing temperature (Fig. 3b).

Changes in the bulk mode resonances indicate the effects of the oxidation treatments on the material away from the edges. The bulk mode of the plasma-oxidized samples shows negligible change (Fig. 2c), while the thermally annealed samples do show changes in their bulk modes (Fig. 2d). When applying the same fitting procedure to the bulk mode, we found little change of H_2 for plasma treated samples but over 20 % change in H_2 for thermally annealed ones, implying a different effect on bulk properties in these two treatments.

While $H_{\rm sat}$ describes the ideality of the edge profile and edge magnetization, the linewidth of the edge resonance reflects the uniformity of the stripe edges. We measure the linewidth of the edge mode by slowly scanning the field around the resonance peak at different frequencies. For samples exposed to oxygen plasma, surprisingly, the linewidth of the edge resonance decreases with moderate edge oxidation as shown in Fig. 3c. The sample with 4 min plasma oxidation shows the minimal linewidth before the linewidth increases again for 10 min oxidation. The linewidth is often modeled as the sum of a term proportional to the damping parameter α and an inhomogeneous broadening term ΔH_0:

$$\mu_0 \Delta H = \mu_0 \Delta H_0 + \frac{1}{\gamma}\frac{4\pi\alpha}{\sqrt{3}} f. \tag{2}$$

Since the change in linewidth merely shows a constant shift rather than a change in slope, Eq. 2 suggests a slight improvement of homogeneity upon oxidation. The SEM image of the stripes reveals a significant amount of short range edge roughness, which has an average amplitude of $\approx$ 10 nm. We speculate that moderate edge oxidation passivates the rough edges, and as a result, reduces the inhomogeneous broadening. The slope obtained from fitting to Eq. 2 corresponds to a damping parameter of $\alpha = 0.006 \pm 0.0002$. We also find that the bulk mode linewidth shows little (less than 1 mT) change for samples treated with plasma for up to 4 min.

In contrast, thermally annealed samples show significant linewidth broadening (Fig. 3d). Except for the sample annealed at 100 °C, the linewidths of samples annealed at higher temperatures show an increase of slope that corresponds to increased damping in the model defined by Eq. 2. The effective damping parameter increases by a factor of 2.2 and 3.7 for 200 °C and 300 °C annealing respectively. The zero frequency offset ΔH_0 displays a large increase for the 300 °C annealing, possibly indicating nonuniformity of edge oxidation from stripe to stripe in the most oxidized sample. Measurement of the bulk mode linewidth reveals a similar, but smaller change of damping parameter. The bulk mode damping increases from $\alpha = 0.006 \pm 0.0004$ for as-grown to 0.008 ± 0.0003 and 0.011 ± 0.0003 for 200 °C and 300 °C annealing (data not shown). Unlike the edge mode, ΔH_0 of the bulk modes was unchanged within the fitting uncertainty.

The oxidation of Py thin films under different oxidation conditions has been investigated by other authors using various methods[15–18]. Both plasma[18] and thermal[15,16] oxidation have been found to result in surface segregation of Fe and formation of iron oxide (Fe_2O_3 or FeO) near the surface. The resultant oxides are either antiferromagnetic or weakly ferromagnetic with little magnetization. However, thermal annealing at temperatures above 200 °C was found to enhance the diffusion of Fe towards the exposed area and lead to a uniform Ni enrichment in the unoxidized bulk material[15,16]. Moreover, annealing at elevated temperatures may also give rise to significant grain growth that facilitates the diffusion of metal species and changes Py structure[16,19].

In the case of edge oxidation, the formed oxides reduce the magnetization near the edges. As a result, the reduction of internal field at the edges due to demagnetization is suppressed, moving the edge mode towards its bulk counterpart. However, for thermally annealed samples, the reduction of magnetization likely extends into the bulk material. The change of bulk mangetization can be seen from the decrease of H_2 for both edge and bulk modes. In addition, the increase of damping at both edges and the bulk film suggests a compositional change in Py stripes upon thermal treatment. We speculate that unlike moderate plasma oxidation in which only the edge magnetization is reduced, thermal annealing above 200 °C has a profound impact on both edge and bulk magnetization due to the promotion of Fe diffusion.

IV. MICROMAGNETIC MODELS

Based on the assumption that plasma and thermal oxidation result in different oxidation profiles, we develop two computational models of oxidation, one where the magnetization is reduced only at the edges, and one where the magnetization is reduced across the stripe.

The details of the micromagnetic calculations[20] include 500 nm by 20 nm overall stripe cross sections and a baseline magnetization $M_{\rm s} = 800$ kA/m. The exchange length value $l_{\rm ex} = 5.69$ nm is held constant in both cases. Keeping either the exchange length or the exchange stiffness constant gives similar results in the simulation. We use a ground-pulse-ring and Fourier transform method to determine the edge mode frequencies for a range of applied fields[21,22], and we determine model values of $H_{\rm sat}$ and H_2 by fitting to Eq. 1. A correction of 13 mT is included in the model results to account for static field differences between single stripe and a stripe array.

To model oxidation of the edge surfaces, we create a gradient in $M_{\rm s}$ such that it decreases linearly over a distance D from its bulk value of 800 kA/m to zero at the physical edges. The results of this model are shown in Fig. 4, where the upper set of model points shows a decrease in $H_{\rm sat}$ and an increase in H_2 as the dilution

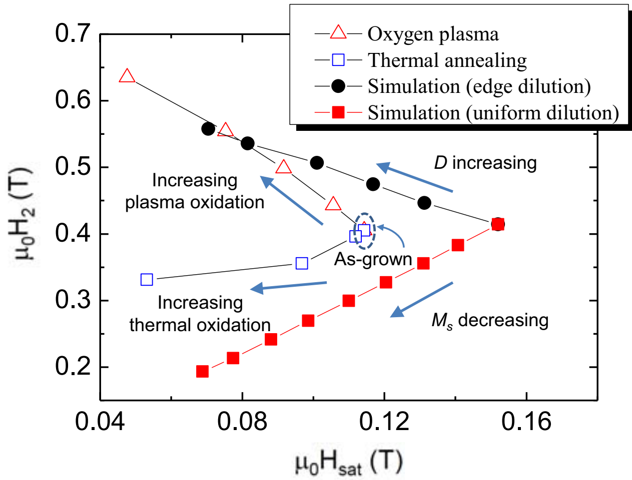

FIG. 4: (Color online) $\mu_0 H_2$ vs $\mu_0 H_{\mathrm{sat}}$. Hollow symbols are experimental data and solid symbols are micromagnetic simulations.

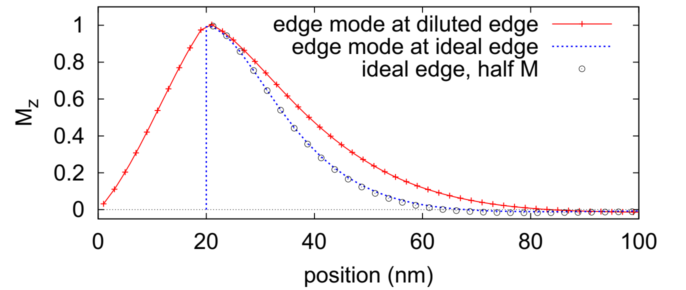

FIG. 5: (Color online) Edge mode profiles calculated in stripes with different models of edge oxidation. The dotted curve is the edge mode profile for an ideal edge placed at 20 nm. The points give the mode profile for a stripe with M_{s} reduced by half, also with the edge placed at 20 nm. The top curve is the edge mode profile when the magnetization increases linearly from zero at 0 nm to full value at D = 20 nm. This edge dilution causes the edge mode to be less strongly localized.

length is varied from $D = 6$ nm to $D = 40$ nm, following the trend found in the plasma oxidized samples.

We separately model the effects of oxidation on the interior of the film by fixing the edge dilution distance at $D = 6$ nm and varying M_{s} so that the magnetization values in the interior of the stripe and in the edge region are reduced proportionally. We justify the reduction of M_{s} in our model by noting that H_2 of the bulk mode drops by 20% under thermal oxidation, and attributing this effect to reduction of M_{s} in the bulk due to preferential oxidation of high-moment Fe atoms, as indicated by refs.[15,16]. Further, we note that the edge surface is not protected by the alumina capping layer, so we expect stronger oxidation effects at the edge. While the measurements indicate a possible 20% reduction of M_{s} in the bulk, for the purposes of modeling the edge mode behavior, we model up to a 50% reduction in M_{s}. The lower set of model points in Fig. 4 shows the effect of decreasing M_{s} from 800 kA/m to 400 kA/m, which creates a decrease in both H_{sat} and H_2, loosely following the trend observed in the thermally annealed samples.

The reduction of H_{sat} for both oxidation models is expected from the fact that H_{sat} is primarily a magnetostatic effect. Since both methods reduce the magnetization at edges, they also therefore reduce the magnetostatic fields at the film edges[11]. The reduction of H_2 due to uniform reduction of M_{s} in the second model is also expected for similar reasons. Contrary to these trends, however, H_2 increases when only the edge magnetization is diluted as seen in the first model.

Some insight into the increases in H_2 with edge magnetization dilution can be gained by looking at the profiles of the edge modes. Fig. 5 compares the edge mode precession profiles calculated for an ideal edge with uniform M_{s} = 800 kA/m and representative examples of our two edge oxidation models, an edge oxidation model with dilution depth D = 20 nm and full magnetization M_{s} = 800 kA/m away from the edges, and a bulk oxidation model with uniform M_{s} = 400 kA/m and no edge dilution (D = 0 nm). The striking result of this comparison is that the uniform reduction of M_{s} has very little effect on the mode profile, while dilution of the magnetization near the edge results in a less strongly localized mode.

The broader mode profile of the edge mode in the films with diluted edges is consistent with higher values of H_2. As the mode profile extends deeper into the film, the effective out-of-plane demagnetization fields would be expected to increase. Indeed, in the limit of a very broad, delocalized mode, we expect that values of H_2 would approach the value seen in the bulk modes, and this is just the behavior observed experimentally for H_2 values in the plasma oxidized films (Fig. 3a).

Although the simulations show a larger H_{sat} than the experimental values, the predicted changes of H_{sat} and H_2 qualitatively agree with the experimental data. It is reasonable to believe that the bulk magnetization in thermally annealed samples has been compromised to some extent. This change in magnetization is possibly due to thermally activated diffusion of Fe atoms or structural modifications in Py stripes at elevated temperatures.

V. SUMMARY

In summary, we measured the magnetic properties of $Ni_{80}Fe_{20}$ stripe edges subjected to two oxidation processes. In both cases, the edge saturation field decreases with increasing oxidation, indicating a reduction of edge magnetization. For some technological applications, smaller demagnetization field near the edges is desirable since it makes magnetization rotation in the structure nearly uniform and reduces the switching field distribution[5]. In these cases, oxidation is helpful in re-

ducing the edge magnetization. However, excessive oxidation is undesirable, especially if the oxidation changes the damping parameter. In this sense, oxygen plasma treatment has the advantages of reducing edge magnetization while keeping damping properties and bulk composition intact. By careful control of plasma treatment time, even homogeneity could be improved by passivating rough edges. On the other hand, to achieve a similar reduction of H_{sat}, thermal oxidation at elevated temperature shows detrimental effects possibly due to altered Py composition throughout the stripes.

Acknowledgments

We thank Gerard Henein, Lei Chen, Michael Hernandez, Marc Cangemi for help with fabrication. And we thank Paul Morrow for oxidation recipes and John Read for allocating FMR instrument time. This work has been supported in part by the NIST-CNST/UMD-Nanocenter Cooperative Agreement.

---

* Electronic address: meng.zhu@nist.gov
† Electronic address: robert.mcmichael@nist.gov

[1] M. Herrmann, S. McVitie, and J. H. Chapman, J. Appl. Phys. **87**, 2994 (2000).
[2] J. G. Deak and R. H. Koch, J. Magn. Magn. Mater. **213**, 25 (2000).
[3] M. T. Bryan, D. Atkinson, and R. P. Cowburn, Appl. Phys. Lett. **85**, 3510 (2004).
[4] O. Ozatay, P. G. Gowtham, K. W. Tan, J. C. Read, K. A. Mkhoyan, M. G. Thomas, G. D. Fuchs, P. M. Braganca, E. M. Ryan, K. V. Thadani, et al., Nature Materials **7**, 567 (2008).
[5] M. Yoshikawa, S. Kitagawa, S. Takahashi, T. Kai, M. Amano, N. Shimomura, T. Kishi, S. Ikegawa, Y. Asao, H. Yoda, et al., J. Appl. Phys. **99**, 08R702 (2006).
[6] J. R. Childress and R. E. Fontana, Comptes Rendus Physique **6**, 997 (2005).
[7] J. Slaughter, R. Dave, M. DeHerrera, M. Durlam, B. Engel, J. Janesky, N. Rizzo, and S. Tehrani, J. of superconductivity **15**, 19 (2002).
[8] J. Jorzick, S. O. Demokritov, B. Hillebrands, M. Bailleul, C. Fermon, K. Y. Guslienko, A. N. Slavin, D. V. Berkov, and N. L. Gorn, Phys. Rev. Lett. **88**, 047204 (2002).
[9] J. P. Park, P. Eames, D. M. Engebretson, J. Berezovsky, and P. A. Crowell, Phys. Rev. Lett. **89**, 277201 (2002).
[10] B. B. Maranville, R. D. McMichael, S. A. Kim, W. L. Johnson, C. A. Ross, and J. Y. Cheng, J. Appl. Phys. **99**, 08C703 (2006).
[11] R. D. McMichael and B. B. Maranville, Phys. Rev. B **74**, 024424 (2006).
[12] M. E. Walsh, Ph.D. thesis, Massachusetts Institute of Technology (2004).
[13] R. Hsiao, D. Miller, and A. Kellock, J. vac. sci. technol. A **14**, 1028 (1996).
[14] B. B. Maranville, R. D. McMichael, and D. W. Abraham, Appl. Phys. Lett. **90**, 232504 (2007).
[15] W.-Y. Lee, G. Scherer, and C. R. Guarnieri, J. Electrochem. Soc. **126**, 1533 (1979).
[16] W. Brückner, S. Baunack, M. Hecker, J. Thomas, S. Groudeva-Zotova, and C. M. Schneider, Mater. Sci. Eng. B **86**, 272 (2001).
[17] M. R. Fitzsimmons, T. J. Silva, and T. M. Crawford, Phys. Rev. B **73**, 014420 (2006).
[18] R. Hsiao and D. Mauri, Appl. Surf. Sci **157**, 185 (2000).
[19] F. Czerwinski, J. A. Szpunar, and U. Erb, J. Mat. Sci.: Materials in Electronics **11**, 243 (2000).
[20] M. J. Donahue and D. G. Porter, in *Interagency Report NISTIR 6376* (National Institute of Standards and Technology, Gaithersburg, MD, 1999).
[21] O. Gérardin, H. Le Gall, M. J. Donahue, and N. Vukadinovic, J. Appl. Phys. **89**, 7012 (2001).
[22] R. D. McMichael and M. D. Stiles, J. Appl. Phys **97**, 10J901 (2005).